Int J Biometeorol (2017) 61:189–198
DOI 10.1007/s00484-016-1203-2

ORIGINAL PAPER

Comparison of selected approaches for urban roughness determination based on voronoi cells

Christine Ketterer[1,2] · Marcel Gangwisch[2] · Dominik Fröhlich[2] · Andreas Matzarakis[3,4]

Received: 8 January 2016 / Revised: 14 May 2016 / Accepted: 13 June 2016 / Published online: 1 July 2016

Abstract Wind speed is reduced above urban areas due to their high aerodynamic roughness. This not only holds for above the urban canopy. The local vertical wind profile is modified. Aerodynamic roughness (both roughness length and displacement height) therefore is relevant for many fields within human biometeorology, e.g. for the identification of ventilation paths, the concentration and dispersion of air pollutants at street level or to simulate wind speed and direction in urban environments and everything depending on them. Roughness, thus, also shows strong influence on human thermal comfort. Currently, roughness parameters are mostly estimated using classifications. However, such classifications only provide limited assessment of roughness in urban areas. In order to calculate spatially resolved roughness on the micro-scale, three different approaches were implemented in the SkyHelios model. For all of them, the urban area is divided into reference areas for each of the obstacles using a voronoi diagram. The three approaches are based on building and [+one of them also on] vegetation (trees and forests) data. They were compared for the city of Stuttgart, Germany. Results show that the approach after Bottema and Mestayer (J Wind Eng Ind Aerodyn 74–76:163–173 1998) on the spatial basis of a voronoi diagram provides the most plausible results.

Keywords Roughness length · Displacement height · Voronoi diagram · SkyHelios · Stuttgart

✉ Dominik Fröhlich
dominik.froehlich@meteo.uni-freiburg.de

Christine Ketterer
ketterer@ima-umwelt.de

Marcel Gangwisch
marcel.gangwisch@saturn.uni-freiburg.de

Andreas Matzarakis
andreas.matzarakis@dwd.de

1 iMA Richter & Röckle, Eisenbahnstrasse 43, 79098 Freiburg, Germany

2 Chair of Environmental Meteorology, Albert-Ludwigs-University of Freiburg, Werthmannstraße 10, 79085 Freiburg, Germany

3 Research Center Human Biometeorology, Deutscher Wetterdienst, Stefan-Meier-Str. 4, 79104 Freiburg, Germany

4 Faculty of Environment and Natural Resources, Albert-Ludwigs-University Freiburg, 79085 Freiburg, Germany

Introduction

Human-thermal conditions are analyzed in cities all over the world in order to assess the prevailing microclimate and to quantify mitigation and adaptation measures (Jendritzky et al. 2012; Johansson and Emmanuel 2006; Lin and Matzarakis 2008; Fröhlich and Matzarakis 2013; Charalampopoulos et al. 2013, 2015). Latest approaches derive spatially resolved micro-meteorological maps visualizing, e.g. the intensity of the urban heat island as well as human thermal comfort (Ketterer and Matzarakis 2014a, b). The effect of meteorological conditions on human beings is often quantified using thermal indices based on the human energy balance (Gagge et al. 1986; Höppe 1999; Fanger and Toftum 2002). Thermal indices, e.g. physiologically equivalent temperature (PET) (Mayer and Höppe 1987; Höppe 1999; Matzarakis et al. 1999) or universal thermal climate index (UTCI, (Bröde et al. 2012; Havenith et al. 2012)), are based on the meteorological parameters air temperature, air humidity, and mean radiant temperature summarizing the short- and long-wave radiation fluxes, as well as wind speed. The meteorological variables are often measured at heights (e.g. at a height of 7 to 10 m or at roof top level) differing from the target height (compare to, e.g. Matzarakis et al. (2009) and Fröhlich and Matzarakis (2013)). Therefore, the meteorological variables need to be vertically extrapolated to the area of interest. While variations in air temperature and air humidity over small distances often range within the accuracy of measurements, wind speed and direction vary strongly in urban surroundings. In order to calculate thermal indices, wind speed at the height of the human gravity center in 1.1 m aboveground ($v_{1.1}$) is required (Matzarakis et al. 2009). For the calculation of most thermal indices (e.g. PET), thus, an altitude correction to $v_{1.1}$ is required:

$$v_{1.1} = v_h \cdot \frac{1.1}{h}^{\alpha} \tag{1}$$

where v_h is the wind speed (ms^{-1}) at a height h and α is an empirical exponent

$$\alpha = 0.12 \cdot z_0 + 0.18 \tag{2}$$

For most approaches using a vertical profile, the roughness length (z_0) is required. More sophisticated vertical profiles (e.g. the urban canopy profile after Macdonald (2000)) also require the displacement height (z_d). These values have to be selected carefully, as they affect wind speed, which influences most thermal indices strongly (e.g. for PET, refer to Table 1).

The wind field itself is strongly modified by urban structures through their high aerodynamic roughness (Landsberg 1981). The average wind speed is generally reduced within cities compared to their rural surroundings as surface roughness serves as a momentum sink (Wieringa 1993). Aerodynamic roughness depends on surface drag and turbulence intensity, describing the effectivity of a surface in transferring parts of the laminar motion energy to turbulent motion within the surface boundary layer (Davenport et al. 2000).

Table 1 Exemplary calculations to demonstrate the influence of wind speed on PET. All results are in degrees Celsius. Calculations were performed assuming a constant relative humidity (RH) of 60 %, air temperature (T_a) constantly equal to the mean radiant temperature (T_{mrt}) and wind speed (v) according to the values on the right hand side of the table

T_{mrt} = T_a (°C)	v = 0.5 m/s	1.0 m/s	3.0 m/s	5.0 m/s	10.0 m/s
0.0	−2.9	−4.3	−6.4	−7.2	−8.1
20.0	18.3	17.2	15.4	14.6	13.8
30.0	29.9	29.4	28.4	27.7	26.7

Roughness (both the roughness length (z_0) and the displacement height (z_d)) is also relevant in other meteorological fields, e.g. wind field modelling used in wind energy, and evaporation analysis (Wieringa 1993; Grimmond and Oke 1999; Gál et al. 2009).

Roughness can be assessed by anemometric or micrometeorological measurements in at least three different heights. These measurements can be used to estimate a logarithmic wind profile allowing for the computation of the roughness length z_0:

$$\bar{u}(z) = \frac{u_*}{\kappa} \cdot \ln\left(\frac{z}{z_0}\right) \tag{3}$$

The logarithmic wind profile describes the vertical development of wind speed $\bar{u}(z)$ along height z within the Prandtl layer. Von Karman's constant (κ) is a dimensionless constant of approximately 0.4. The friction velocity u_* indicates the present turbulence that is constant with height in the Prandtl layer. However, this data is often unavailable, measurements are expensive and the methodology is error-prone in urban areas (Gál and Unger 2009). Therefore, roughness approximation based on urban morphology is a more applicapable substitute. Extensive reviews about roughness estimation have been published by Counihan (1975), Wieringa (1993), Grimmond et al. (1998), and Grimmond and Oke (1999).

The roughness classifications by Davenport et al. (2000) are often used in applied science, e.g. for the determination of the "Local Climate Zone" (Stewart and Oke 2012). It consists of eight classes. Only two of them are representing settlements and urban areas, which are not distinguished any further.

The most common parameters for the assessment of roughness are the zero-plane displacement height (z_d), the roughness length (z_0) and the drag coefficient $C_{D(z)}$ (Lettau 1969; Counihan 1975; Wieringa 1993). Their calculation is usually based on the frontal area density (λ_f) and the building plan area density (λ_p) (Bottema 1997; Bottema and Mestayer 1998; Grimmond and Oke 1999). Alternative ways to describe roughness are the effective height (h_{eff}) (Matzarakis and Mayer 1992), the porosity of the urban canopy layer (P) or the urban directionality (Compagnon and Raydan 2000; Ratti et al. 2006). Roughness caused by an obstacle is calculated based on its geometry and its specific reference area. Each reference area has to be dedicated to an individual obstacle in order to quantify the obstacle's aerodynamic roughness. Up to now, the area of interest usually is split up into a rectangular grid (Matzarakis and Mayer 1992), lot areas (Gál et al. 2009) or other arbitrary reference areas (Ratti et al. 2006). The methodology proposed in this study applies a voronoi diagram (also called Dirichlet tessellation or Thiessen polygon) to determine the reference area of buildings and trees in cities.

The aim of the paper is to propose a new methodology to determine spatially resolved roughness information based on morphological data. Three different approaches to calculate roughness (Lettau 1969; Matzarakis and Mayer 1992; Bottema and Mestayer 1998) are compared for an area in Stuttgart, Germany, that serves as a case study.

Methods and data

Voronoi diagramm

Splitting the study area into reference areas, which is required for all the approaches for roughness calculation, has to be done very carefully, as their size influences the results significantly. A voronoi diagram was selected as the determination method of the reference areas. A voronoi diagram $VD(X)$ of a point set X is the segmentation of the two-dimensional space (Euclidean plane) into voronoi cells $VC_{\text{point}}(x) : x \in X$. A voronoi cell $VC_{\text{point}}(p)$ is the geometric area containing point p, which is located closer to p than to any other point $x \in X \setminus \{p\}$ (Ottmann and Widmayer 2012).

To calculate a voronoi cell for a set of polygons (Y), the location of all points in the Euclidean plane has to be closer to polygon q than to any other polygon $y \in Y \setminus \{q\}$. The polygon q's voronoi cell $VC_{\text{polygon}}(q)$ is determined by the union of all voronoi cells ($VC_{\text{point}}(o)$) of all points on the outline of polygon q, $VC_{\text{point}}(o) : o \in q$.

$$VC_{\text{polygon}}(q) = \bigcup_{o \in q} VC_{\text{point}}(o) \tag{4}$$

$VC_{\text{polygon}}(q)$: voronoi cell for polygon q
$VC_{\text{point}}(o)$: voronoi cell for point o
o: point on the outline of polygon q

Figure 1 shows an example of a study area divided into reference areas considering buildings and trees.

The calculation of the voronoi diagram was done with the fastest Fortune's algorithm (Fortune 1987) with a runtime complexity of $O(n \log n)$ for single points. In order to use the algorithm for polygons, they are dissolved in single points bordering each polygon.

Roughness calculation

This study is following three different approaches of roughness calculation applied for every voronoi cell: the

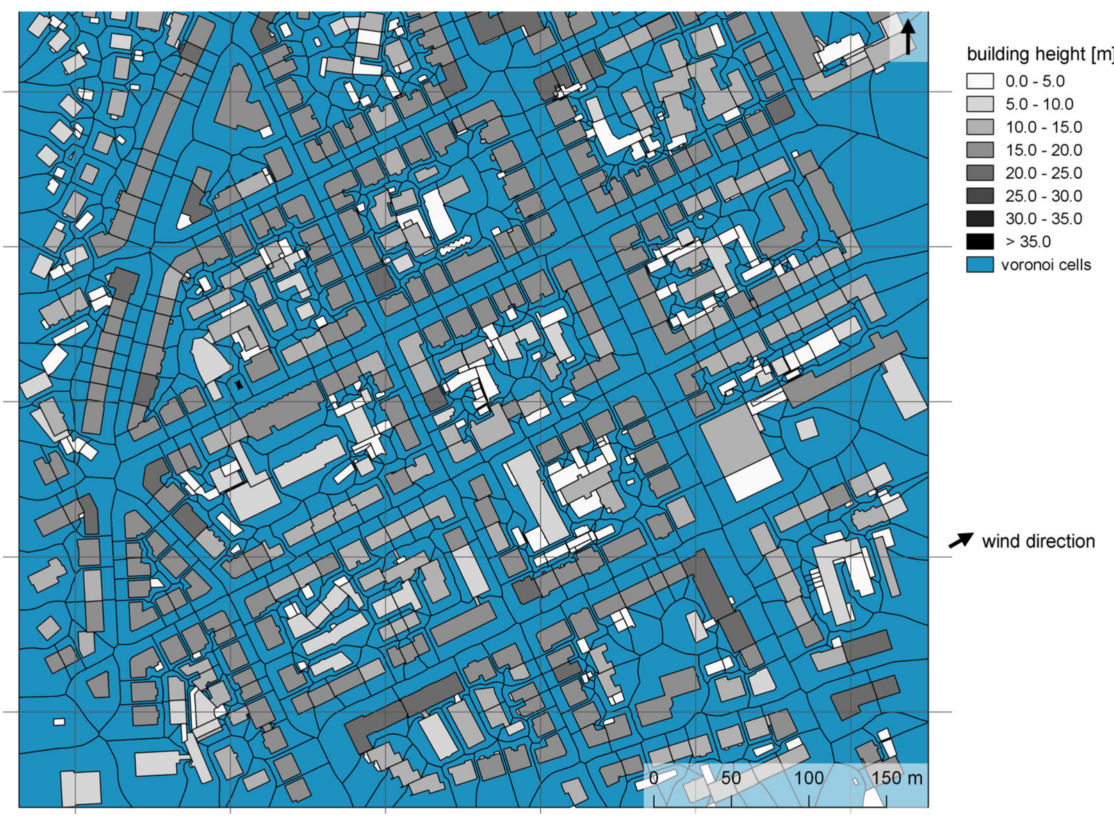

Fig. 1 Voronoi diagram with individual cells for each building and tree

morphometric approach (Lettau 1969), effective heights (Matzarakis and Mayer 1992) and an approach after Bottema and Mestayer (1998). For an overview of the three approaches, refer to Table 2.

Morphometric approach after Lettau

Lettau (1969) developed an approach based on observations for irregular arrays of homogeneous roughness elements. He proposed a method to calculate aerodynamic roughness length z_o depending on the average height (h^*), the frontal area (A_{frontal}) and the reference area (A_{total}):

$$z_0 = 0.5 \cdot \lambda_{\mathrm{f}} \cdot h^* \tag{5}$$

with

$$\lambda_{\mathrm{f}} = A_{\mathrm{frontal}} \cdot A_{\mathrm{total}}^{-1} \tag{6}$$

As this approach is based on the frontal area, it also depends on the wind direction (also refer to Table 2).

Effective heights

Matzarakis and Mayer (1992) defined in their approach the "effective heights" (h_{eff}) which is defined as the sum of the averaged and weighted height of buildings, vegetation and other objects for grid points. The averaged heights of buildings, vegetation and other surfaces for each reference area are weighted by the occupied area.

$$h_{\mathrm{eff}} = \lambda_{\mathrm{p,B}} \cdot h_{\mathrm{B}} + \lambda_{\mathrm{p,V}} \cdot h_{\mathrm{V}} + \lambda_{\mathrm{p,S}} \cdot h_{\mathrm{S}} \tag{7}$$

where

$\lambda_{\mathrm{p,B}}$: plan area density for buildings
h_{B}: average building height (m)
$\lambda_{\mathrm{p,V}}$: λ_{p} for vegetation
h_{V}: average vegetation height (m)
$\lambda_{\mathrm{p,S}}$: λ_{p} for all other surfaces inside reference area
h_{S}: average height of the other surfaces (m)

This approach is independent of incident wind direction (Table 2).

To be able to compare the results after Matzarakis and Mayer (1992) to those calculated by the other two approaches, the relationship

$$z_0 = 0.25 \cdot h_{\mathrm{eff}} \tag{8}$$

is assumed as proposed by Kondo and Yamazawa (1986).

Approach after Bottema (1997) and Bottema and Mestayer (1998)

Bottema (1997) published an approach based on the frontal vortex zone and the recirculation zone in the lee of an obstacle. As these values are not available, the roughness length z_0 is calculated depending on the volumetric average of the obstacle's height h, the frontal area density λ_{f} and the plan area density λ_{p} (Bottema and Mestayer 1998).

$$z_0 = (h_{\mathrm{v,i}} - z_{\mathrm{d}}) \exp\left(-\frac{\kappa}{\sqrt{0.5 C_{\mathrm{Dh}} \lambda_{\mathrm{f}}}}\right) \tag{9}$$

where κ is the von Karman constant (0.4), C_{Dh} is an isolated obstacle drag coefficient and λ_{f} is the frontal area density. The zero-plane displacement height (z_{d}) is calculated by the volumetric average obstacle height h_{i} and the planar area density λ_{p}. Using this equation, C_{Dh} is considered constant (Bottema and Mestayer 1998).

$$z_{\mathrm{d}} = h_{\mathrm{i}} \cdot \lambda_{\mathrm{p}}^{0.6} \tag{10}$$

Considering not only buildings but also trees and forests, their z_{d} is calculated including their porosity P. The zero-plane displacement height for forests was calculated by

$$z_{\mathrm{d,forest}} = 0.66 \cdot h_{\mathrm{forest}} \tag{11}$$

Brutsaert (1975) and for trees with [-base +an] area A_{tree} [+covered by the tree crown] (Grimmond and Oke 1999):

$$z_{\mathrm{d}} = h_{\mathrm{i}} \cdot \left(\frac{(1 - P_{\mathrm{tree}}) A_{\mathrm{tree}}}{A_{\mathrm{total}}}\right)^{0.6} \tag{12}$$

The drag coefficient C_{Dh} is afterwards reduced by $C_{\mathrm{Dh}} \cdot (1 - P)$ for trees and forests. Porosity values are individual

Table 2 Overview over the different approaches and the parameters they are based on. All approaches are determined by the size of the voronoi cell (VC_i) and the obstacle's height (h_i). Some of them also depend on wind direction (WD), the obstacle's planar area (A_i) or the drag coefficient (C_{Dh})

Approach	Equation	Determinants
Morphometric approach after Lettau (1969)	$z_0 = 0.5 \cdot \frac{1}{A_{\mathrm{total}}} \cdot A_{\mathrm{frontal}} \cdot h^*$	VC_i, WD, h_i
Effective height after Matzarakis and Mayer (1992) and Mayer and Matzarakis (1992)	$h_{\mathrm{eff}} = \lambda_{\mathrm{p,B}} \cdot h_{\mathrm{B}} + \lambda_{\mathrm{p,V}} \cdot h_{\mathrm{V}} + \lambda_{\mathrm{p,S}} \cdot h_{\mathrm{S}}$	VC_i, A_i, h_i
Approach after Bottema (1997) and Bottema and Mestayer (1998)	$z_0 = (h_{\mathrm{v},i} - z_{\mathrm{d}}) \exp\left(-\frac{\kappa}{\sqrt{0.5 C_{\mathrm{Dh}} \lambda_{\mathrm{f}}}}\right)$	VC_i, WD, A_i, h_i, C_{Dh}

but constant for the whole study area (e.g. 0.99 for *Picea abies* forests, 0.2 for mixed forests and 0.3 for trees).

The frontal area density λ_f is the ratio of the sum of the individual frontal areas $A_{frontal}$ of each obstacle (i) divided by the total reference area A_{total}. λ_f can be calculated for regular and irregular obstacles.

$$\lambda_f = \frac{\sum_{i=0}^{n} A_{frontal,i}}{A_{total}} \tag{13}$$

The frontal area depends on the incident wind direction. If several frontal areas are overlapping, only the parts not covered by other obstacles are considered.

To calculate the frontal area of one building, the coordinate system is rotated according to the wind direction. For that purpose the 2D rotation matrix R_α was applied to rotate every point of the obstacle by the angle α around the origin. The frontal area is calculated as the product of the building height times the distance between the smallest and largest value on the x-axis (compare to Fig. 2).

The planar area density (λ_p) is the ratio of the sum of individual planar areas (projected roof area) A_{planar} of each obstacle (i) compared to the whole reference area A_{total}.

$$\lambda_p = \frac{\sum_{i=0}^{n} A_{planar,i}}{A_{total}} \tag{14}$$

The volumetric height $h_{v,i}$ is the sum of the product of each obstacle's volume V_i and height h_i divided by the sum of the volume of all the individual obstacles.

$$h_{v,i} = \frac{\sum_{i=0}^{n} V_i \cdot h_i}{\sum_{i=0}^{n} V_i} \tag{15}$$

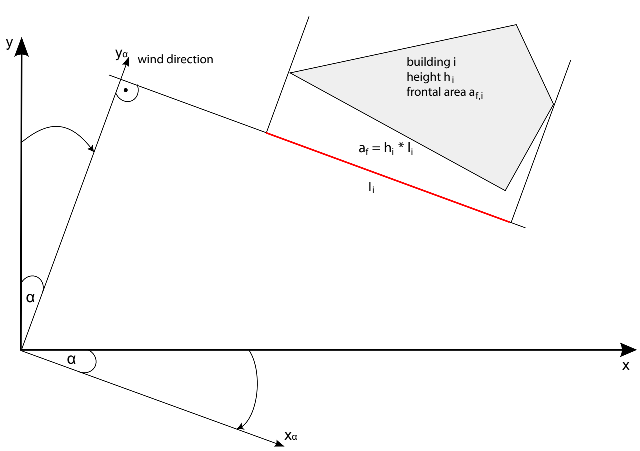

Fig. 2 Rotated coordinate system for the calculation of the frontal area of a building

SkyHelios

SkyHelios (Matzarakis and Matuschek 2011) is a micro-scale model for the calculation of micro-meteorological conditions in complex urban environments. It is developed with run-time efficiency and reduction of costs by the use of free and open-source third-party software in mind. SkyHelios allows for the calculation of meteorological and auxiliary parameters, e.g. Sky View Factor, shading, sunshine duration, mean radiant temperature, wind speed and wind direction. This information is used to calculate thermal indices (e.g. physiologically equivalent temperature (Mayer and Höppe 1987) and universal thermal climate index (Bröde et al. 2012; Havenith et al. 2012)). Results can be obtained for single points as well as for the whole model area. Based on the GDAL library (Open Source Geospatial Foundation 2016), SkyHelios supports raster and vector data in all the common file formats used by Geographic Information Systems (GIS). Several files can be loaded and are considered in correct relative orientation, if the spatial reference system (SRS) is specified correctly. The imported spatial data is displayed three-dimensionally by using the 3D graphics engine Mogre (MOGRE Community 2016). Spatial results are returned as ASCII grids, which are supported by most of the commercial or open-source GIS for display and further processing.

Brief description of the study area

The study area, Stuttgart, is located in the south-western part of Germany in complex topography. Stuttgart's city center is located in a basin, while most districts are spread over the surrounding hills and valleys. In the basin, the area is densely built-up but also comprises some parks, whereas along the ridge, the most common land use type is forest.

Results and discussion

Voronoi cells

Surface roughness calculation depends on the land cover type and its extensions. Therefore, the surface area has to be divided. This could be done using a regular grid or voronoi cells.

Using a regular raster grid, the resolution would play an important role: a low resolution would lead to an averaged roughness length, which is not suitable for micro-scale analysis. If the resolution is high, it might result in many grids without any roughness elements while all neighbour cells contain roughness objects. The roughness length at grids without roughness elements would be low roughness resulting in an overestimation of wind speed.

Voronoi cell area is of advantage because it considers single objects as forests, single trees and buildings. Thus, the spatial resolution depends on the relation between the number of objects and the plane surface area. In cities, the size of a voronoi cell describes the space of a building. The resulting high resolution of the voronoi cells and the roughness calculation are suitable for micro-scale analysis of the human bioclimate and to transfer wind measurements from the measuring site to the study area. Furthermore, voronoi cells consider planar areas and building density. However, if the input data distinguishes various roof heights of one building by different polygons, voronoi cells become very small. Such small reference areas lead to an overestimation of the aerodynamic surface roughness. Therefore, all polygons of one building are combined and the building height is averaged weighted by the volume of each polygon.

Roughness length

Figure 3 shows the roughness length z_0 calculated for Stuttgart using the approach of Lettau (1969) for the prevailing wind direction of 240°. The approach takes wind direction but not z_d into account. This leads to very high values of z_0 compared to the approaches after Matzarakis and Mayer (1992) and Bottema and Mestayer (1998) (compare to Figs. 4 and 5). Especially row houses in an orientation perpendicular to the incident wind direction lead to very high values of z_0 after Lettau (1969).

Figure 4 shows the roughness length z_0 calculated for Stuttgart using the approach of Matzarakis and Mayer (1992). In the approach after Matzarakis and Mayer (1992), the wind direction is not considered. This leads to a more homogeneous distribution of the effective heights (also refer to Fig. 6). Throughout the area of interest, the calculated effective heights are higher than z_0 calculated by the other two approaches. If the relationship after Eq. 8 is assumed, the approach after Matzarakis and Mayer (1992) returns slightly lower results than the one after Lettau (1969), but higher ones than Bottema and Mestayer (1998) (compare colors in Figs. 3, 4, and 5).

Figure 5 shows the roughness length z_0 calculated for Stuttgart using the approach of Bottema and Mestayer (1998) for the prevailing wind direction of 240°. The consideration of the wind direction leads to a reduced z_0 for buildings parallel to the incident wind direction. Due to the consideration of z_d, the approach after Bottema and Mestayer (1998) returns the lowest values for z_0 compared to the other two approaches (see Figs. 3 and 4).

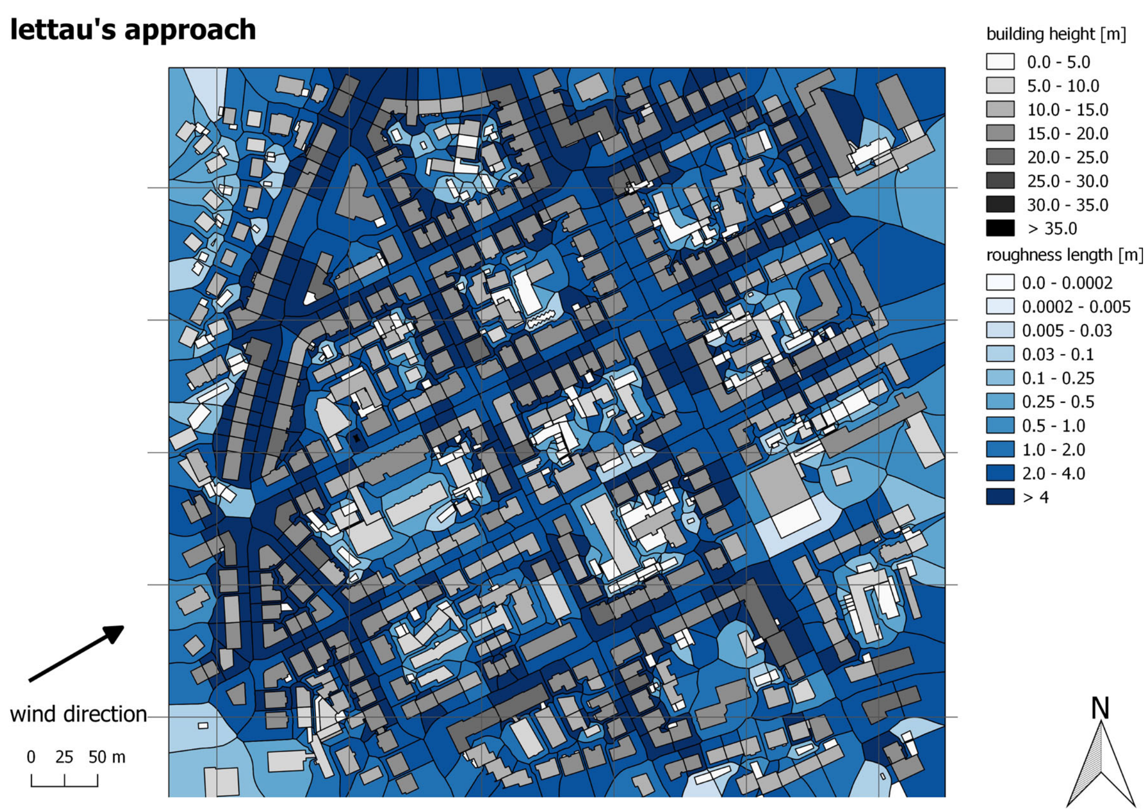

Fig. 3 Building height and roughness length calculated for the South-Western part of Stuttgart using the approach of Lettau (1969) for the wind direction of 240 °

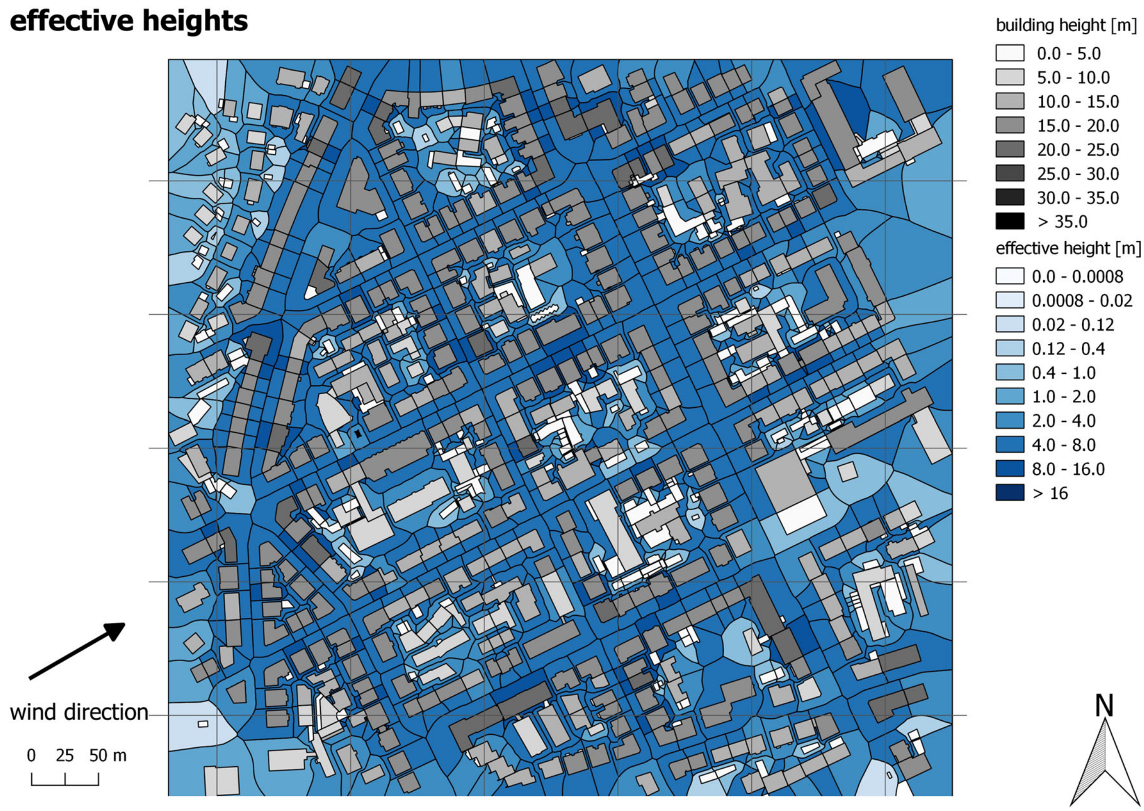

Fig. 4 Building height and roughness length calculated for the South-Western part of Stuttgart using the approach of Matzarakis and Mayer (1992). Wind direction is not considered in this approach

Comparing the approach of Lettau (1969) to the one of Matzarakis and Mayer (1992) assuming $z_0 = 0.25 \cdot h_{\mathrm{eff}}$ as applied by Kondo and Yamazawa (1986), it can be found that in large reference areas $h_{\mathrm{eff}} \succ\succ z_0$ and in a densely built-up area $h_{\mathrm{eff}} \prec\prec z_0$ (see Figs. 3 and 4). The standard deviation between the two approaches within the area of interest is 1.81 m, the variance 3.3. The advantage of the effective heights approach is the consideration of vegetation, although a consideration of porosity is missing (as proposed e.g. by Grimmond and Oke (1999)).

In both approaches z_d is not considered. However, when the plan area density is larger than 20-30 %, mutual sheltering of the obstacles becomes the prevailing influence. Below the displacement height, the flow regime is changed to turbulent, while it stays laminar above. Therefore, the approaches by Lettau (1969) and Matzarakis and Mayer (1992) can only be used for study areas without a zero-plane displacement (Macdonald et al. 1998; Grimmond and Oke 1999; Davenport et al. 2000). To meet this shortcoming, the effective heights approach could be modified to

$$h_{\mathrm{eff}} = \lambda_{p,B} \cdot (h_B - z_{d,B}) + \lambda_{p,V} \cdot (h_V - z_{d,V}) + \lambda_{p,S} \cdot (h_S - z_{d,S}) \quad (16)$$

Bottema and Mestayer (1998) already consider vegetation along with its porosity as well as z_d. The standard deviation to the results of Lettau (1969) is 1.57 m, the variance 2.5. The standard deviation to the results calculated using the approach after Matzarakis and Mayer (1992) is 0.64 m and therefore way smaller. Also the variance is much smaller (0.4).

The assessment of approaches for the calculation of z_0 and z_d is challenging. This is because both variables are hardly measurable and mostly determined by modelling. Additionally, as calculations were performed spatially, lots of values need to be assessed. On the other hand, the huge quantity of values allows for statistical assessment methods. To get a first insight on how the approaches are performing, the distribution of the results (both spatial (Figs. 3 to 5) and the overall distribution of values (compare to Fig. 6)) can be checked.

For both methods, the approach after Bottema and Mestayer (1998) returned the most plausible distribution of results for the study area avoiding extrema (compare to Figs. 5 and 6).

The reference area of all three approaches was defined to be a rectangle; the voronoi diagram seems to be more

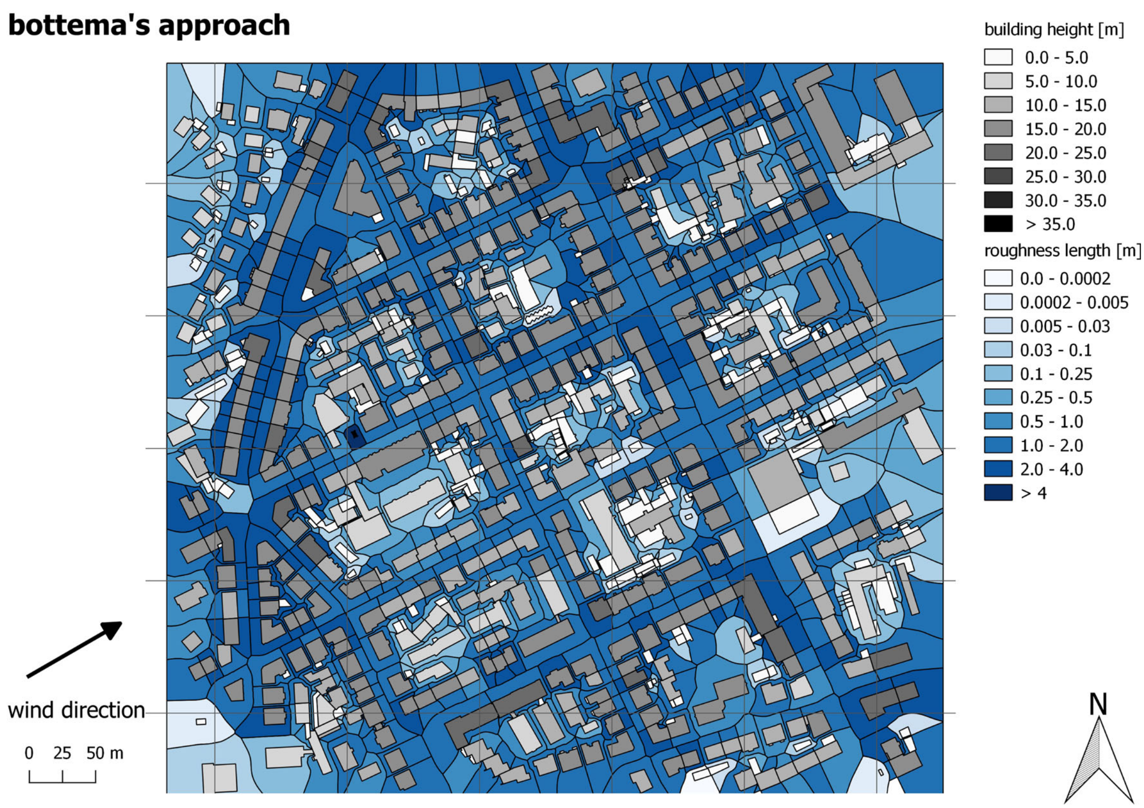

Fig. 5 Building height and roughness length calculated for the South-Western part of Stuttgart using the approach of Bottema and Mestayer (1998) for the wind direction of 240 °

appropriate, as it is dependent on the obstacle's configuration. However, this is a strong modification to the approaches. Results therefore need to be checked for plausibility.

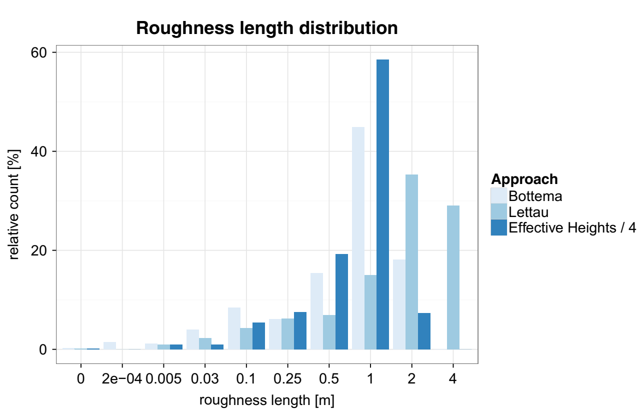

Fig. 6 Frequency distribution of roughness length for the area of investigation estimated by different approaches (see legend). The frequencies are aggregated to the Davenport classes (Davenport et al. 2000)

Conclusion

Roughness length and displacement height show great variability in urban areas. This makes the vertical wind profile and, thus, wind speed in 1.1 m aboveground as required for the calculation of thermal indices like PET vary strongly in space. Local roughness therefore should always be considered if a thermal index is calculated within an urban environment.

The new method for roughness calculation based on voronoi cells as reference areas is shown to allow for more plausible results than recent methods based on rather arbitrary reference areas like lot areas or regular grids.

A new model part was implemented into the SkyHelios model determining the reference area of any obstacle using Fortunes algorithm to calculate a voronoi diagram in a run-time efficient way. Based on that, three approaches were implemented, which now allow for the calculation of the roughness length and displacement height. These can be used to improve the estimation of the wind field.

Each of the three different approaches for roughness calculation based on voronoi cells was applied for the study area in Stuttgart, Germany, and the results were compared. The calculations were based on detailed building and vegetation data.

While the approach after Lettau (1969) only takes urban morphology into account, the effective heights and the approach by Bottema and Mestayer (1998) also allows for the consideration of vegetation in the roughness calculations. Furthermore, in the implementation after Bottema and Mestayer (1998), the porosity of vegetation is considered. This approach therefore is found to be the most suitable for calculation of roughness for urban environments.

Acknowledgments This work is financially supported by the transnational cooperation project 3CE292P3 within the Central Europe Programme "Development and application of mitigation and adaptation strategies and measures for counteracting the global urban heat island phenomenon". This project is implemented through the CENTRAL Europe Programme co-financed by the ERDF.

We thank the Office for Environmental Protection, section of urban climatology of Stuttgart, for providing climate data of Stuttgart Schwabenzentrum and Land Surveying Office, Stuttgart for the spatial data.

Dominik Fröhlich wants to acknowledge the support of the Heinrich-Böll foundation.

References

Bottema M (1997) Urban roughness modelling in relation to pollutant dispersion. Atmos Environ 31(18):3059–3075. doi:10.1016/S1352-2310(97)00117-9

Bottema M, Mestayer PG (1998) Urban roughness mapping—validation techniques and some first results. J Wind Eng Ind Aerodyn 74–76:163–173. doi:10.1016/S0167-6105(98)00014-2

Bröde P, Fiala D, Blazejczyk K, Holmér I, Jendritzky G, Kampmann B, Tinz B, Havenith G (2012) Deriving the operational procedure for the universal thermal climate index (UTCI). Int J Biometeorol 56(3):481–494. doi:10.1007/s00484-011-0454-1

Brutsaert W (1975) Comments on surface roughness parameters and the height of dense vegetation. J Meteorol Soc Japan 53:96–97

Charalampopoulos I, Tsiros I, Chronopoulou-Sereli A, Matzarakis A (2013) Analysis of thermal bioclimate in various urban configurations in Athens, Greece. Urban Ecosyst 16:217–233. doi:10.1007/s11252-012-0252-5

Charalampopoulos I, Tsiros I, Chronopoulou-Sereli A, Matzarakis A (2015) A note on the evolution of the daily pattern of thermal comfort-related micrometeorological parameters in small urban sites in Athens. Int J Biometeorol 59:1223–1236. doi:10.1007/s00484-014-0934-1

Compagnon R, Raydan D (2000) Irradiance and llumination Distributions in Urban Areas Proceedings of the 17th International Conference on Passive and Low Energy Architecture (PLEA) Cambridge, UK

Counihan J (1975) Adiabatic atmospheric boundary layers: a review and analysis of data from the period 1880–1972. Atmos Environ (1967) 9(10):871–905. doi:10.1016/0004-6981(75)90088-8, http://www.sciencedirect.com/science/article/pii/0004698175900888

Davenport AG, Grimmond CSB, Oke TR, Wieringa J (2000) Estimating the roughness of cities and sheltered country. In: 15Th Conference on Probability and Statistics in the Atmospheric Sciences/12th Conference on Applied Climatology, Ashville, NC, American Meteorological Society, pp 96–99

Fanger PO, Toftum J (2002) Extension of the PMV model to non-air-conditioned buildings in warm climates: special issue on thermal comfort standards. Energy Build 34(6):533–536. doi:10.1016/S0378-7788(02)00003-8, http://www.sciencedirect.com/science/article/pii/S0378778802000038

Fortune S (1987) A sweepline algorithm for Voronoi diagrams. Algorithmica 2(1-4):153–174. doi:10.1007/BF01840357

Fröhlich D, Matzarakis A (2013) Modeling of changes in thermal bioclimate: examples based on urban spaces in Freiburg, Germany. Theor Appl Climatol 111:547–558. 10.1007/s00704-012-0678-y

Gagge AP, Fobelets A, Berglund L (1986) A standard predictive index of human response to the thermal environment. ASHRAE Transactions (92, Pt 1):709–731

Gál T, Unger J (2009) Detection of ventilation paths using high-resolution roughness parameter mapping in a large urban area. Build Environ 44(1):198–206. doi:10.1016/j.buildenv.2008.02.008

Gál T, Lindberg F, Unger J (2009) Computing continuous sky view factors using 3D urban raster and vector databases: comparison and application to urban climate. Theor Appl Climatol 95(1-2):111–123. doi:10.1007/s00704-007-0362-9

Grimmond CSB, Oke TR (1999) Aerodynamic properties of urban areas derived from analysis of surface form. J Appl Meteorol 38(9):1262–1292. doi:10.1175/1520-0450(1999)038<1262:APOUAD>2.0.CO;2

Grimmond CSB, King TS, Roth M, Oke TR (1998) Aerodynamic roughness of urban areas derived from wind observations. Bound.-Layer Meteorol 89(1):1–24. doi:10.1023/A:1001525622213

Havenith G, Fiala D, Blazejczyk K, Richards M, Bröde P, Holmér I, Rintamaki H, Benshabat Y, Jendritzky G (2012) The UTCI-clothing model. Int J Biometeorol 56(3):461–470. doi:10.1007/s00484-011-0451-4

Höppe P (1999) The physiological equivalent temperature—a universal index for the biometeorological assessment of the thermal environment. Int J Biometeorol 43(2):71–75. doi:10.1007/s004840050118

Jendritzky G, de Dear R, Havenith G (2012) UTCI—why another thermal index? Int J Biometeorol (56):421–428

Johansson E, Emmanuel R (2006) The influence of urban design on outdoor thermal comfort in the hot, humid city of Colombo, Sri Lanka. Int J Biometeorol 51(2):119–133. doi:10.1007/s00484-006-0047-6

Ketterer C, Matzarakis A (2014a) Comparison of different methods for the assessment of the urban heat island in Stuttgart, Germany. International Journal of Biometeorology. doi:10.1007/s00484-014-0940-3

Ketterer C, Matzarakis A (2014b) Human-biometeorological assessment of heat stress reduction by replanning measures in Stuttgart, Germany. Landsc Urban Plan 122:78–88. doi:10.1016/j.landurbplan.2013.11.003

Kondo J, Yamazawa H (1986) Aerodynamic roughness over an inhomogenous ground surface. Bound.-Layer Meteorol 35(4):331–348. doi:10.1007/BF00118563, wOS:A1986C503200003

Landsberg HE (1981) The urban climate. The Academic Press, London

Lettau H (1969) Note on aerodynamic roughness—parameter estimation on the basis of roughness-element description. J Appl Meteorol 8(5):828–832. doi:10.1175/1520-0450(1969)008<0828:NOARPE>2.0.CO;2

Lin TP, Matzarakis A (2008) Tourism climate and thermal comfort in Sun Moon Lake, Taiwan. Int J Biometeorol 52(4):281–290. doi:10.1007/s00484-007-0122-7

Macdonald RW (2000) Modelling the mean velocity profile in the urban canopy layer. Bound.-Layer Meteorol 97(1):25–45. doi:10.1023/A:1002785830512, wOS:000088631900002

Macdonald RW, Griffiths RF, Hall DJ (1998) An improved method for the estimation of surface roughness of obstacle arrays. Atmos Environ 32(11):1857–1864. doi:10.1016/S1352-2310(97)

Matzarakis A, Matuschek O (2011) Sky view factor as a parameter in applied climatology—rapid estimation by the SkyHelios model. Meteorol Z 20(1):39–45. doi:10.1127/0941-2948/2011/0499

Matzarakis A, Mayer H (1992) Mapping of urban air paths for planning in Munich. In: Planning applications of urban and building climatology Wissenschaftliche Berichte des Instituts für Meteorologie und Klimaforschung Universität Karlsruhe 16

Matzarakis A, Mayer H, Iziomon MG (1999) Applications of a universal thermal index: physiological equivalent temperature. Int J Biometeorol 43(2):76–84. doi:10.1007/s004840050119

Matzarakis A, Rocco M, Najjar G (2009) Thermal bioclimate in Strasbourg—the 2003 heat wave . Theor Appl Climatol 98(3-4):209–220. doi:10.1007/s00704-009-0102-4

Mayer H, Höppe PR (1987) Thermal comfort of man in different urban environments. Theor Appl Climatol 38(1):43–49. doi:10.1007/BF00866252

Mayer H, Matzarakis A (1992) Stadtklimarelevante Luftströmungen im Münchner Stadtgebiet: Forschungsvorhaben STADTLUFT

MOGRE Community (2016) Managed open graphics rendering engine. http://www.ogre3d.org/tikiwiki/MOGRE

Open Source Geospatial Foundation (2016) GDAL: GDAL—Geospatial Data Abstraction Library. http://www.gdal.org/

Ottmann T, Widmayer P (2012) Algorithmen und Datenstrukturen. Springer, Berlin

Ratti C, Di Sabatino S, Britter R (2006) Urban texture analysis with image processing techniques: winds and dispersion. Theor Appl Climatol 84(1-3):77–90. doi:10.1007/s00704-005-0146-z

Stewart ID, Oke TR (2012) Local climate zones for urban temperature studies. Bull Am Meteorol Soc 93(12):1879–1900. doi:10.1175/BAMS-D-11-00019.1

Wieringa J (1993) Representative roughness parameters for homogeneous terrain. Bound-Layer Meteorol 63(4):323–363. doi:10.1007/BF00705357